Molecular Human Reproduction Vol.8, No.11 pp. 1014–1022, 2002

Adhesiveness of human uterine epithelial RL95-2 cells to trophoblast: Rho protein regulation

Carola Heneweer[1], Lars Hendric Kruse[1], Felix Kindhäuser[2], Martina Schmidt[2], Karl H.Jakobs[2], Hans-Werner Denker[1] and Michael Thie[1,3]

[1]Institut für Anatomie and [2]Institut für Pharmakologie, Universitätsklinikum Essen, D-45122 Essen, Germany

[3]To whom correspondence should be addressed. E-mail: michael.thie@uni-essen.de

Embryo implantation involves adhesion of trophoblast cells to the epithelial lining of the endometrium. Using an in-vitro model to simulate this initial interaction, we previously reported that attachment of human trophoblast-like JAR spheroids to human uterine epithelial RL95-2 cells provokes a Ca^{2+} influx in RL95-2 cells depending on apically localized integrin receptors. Here, we demonstrate that adhesiveness of RL95-2 cells for JAR spheroids, measured by a centrifugal force-based adhesion assay, is dependent on Rho GTPases, most likely RhoA. Cellular expression and distribution of RhoA were studied by fluorescence confocal microscopy, focusing on the localization of RhoA and F-actin within the adhesion sites between JAR and RL95-2 cells. Contact areas contained high amounts of RhoA and F-actin fibres near the plasma membrane. To determine whether Rho GTPases may influence JAR cell binding, we treated RL95-2 cells with *Clostridium difficile* toxin A, which specifically inactivates Rho GTPases. Toxin A treatment changed the subcellular distribution of endogenous RhoA in RL95-2 cells and altered RhoA and F-actin colocalization. Adhesion of JAR spheroids to RL95-2 cells treated with toxin A was largely suppressed. These data indicate that Rho GTPases, most likely RhoA, play an important role in uterine epithelial RL95-2 cells for trophoblast binding, and suggest that RhoA may be involved in local signalling cascades during early embryo implantation *in vivo*.

Key words: actin cytoskeleton/adhesion/implantation/Rho GTPases/uterine epithelium

Introduction

Implantation is initiated by adhesion of the embryo to the endometrial mucosa, i.e. the trophoblast of the blastocyst establishes contacts to the free surface of the uterine epithelium, followed by firm adhesion and penetration. For initiation and progression of this process, a state of adhesion competence of the trophoblast (Armant *et al*., 2000) as well as a state of receptivity of the uterine epithelium is required (Denker, 1994; Carson *et al*., 2000; Denker and Thie, 2001).

Acquisition of apical adhesiveness of uterine epithelial cells is apparently the result of a variety of cellular changes, including the protein/glycoprotein composition of the apical plasma membrane, the surface charge, the integrity of the junctional complex and the morphology of the cell surface (Nikas, 1999; Kimber and Spanswick, 2000; Murphy, 2000a,b). These phenomena probably depend specifically on partial down-regulation or destabilization of their polar organization along the apico-basal axis at receptivity (Denker, 1994). Experimental attempts to elucidate details of these processes are largely restricted to animal models as human implantation is inaccessible to such studies. However, in-vitro models using human cell lines simulating the adhesion-competent trophoblast and the receptive uterine epithelium have been developed to obtain, in first order approximation, information about the mechanisms involved. One such model is employed in the present investigation: multicellular spheroids of trophoblastoid JAR cells and monolayers of uterine epithelial RL95-2 cells mimic relevant properties of the adhesion-competent endometrial lining (John *et al*., 1993). In contrast to other endometrial cell lines, RL95-2 cells permanently express a non-polar epithelial phenotype and exhibit adhesiveness of the free pole for trophoblast (Thie *et al*., 1995, 1996). Thus, RL95-2 cells mimic an important aspect of the in-vivo situation and serve as an in-vitro model for the receptive human uterine epithelium (Raboudi *et al*., 1992; John *et al*., 1993; Rhode and Carson, 1993; Thie *et al*., 1995, 1996, 1997, 1998; Liu *et al*., 1998; Chervenak and Illsley, 2000; Hohn *et al*., 2000; Martin *et al*., 2000; Tinel *et al*., 2000; Perret *et al*., 2001).

We have previously studied certain mechanisms involved in formation of cell–cell contacts between uterine epithelial cells and trophoblast in this in-vitro model. We demonstrated that this time-dependent process includes sequential steps of bond formation as well as complex signal transduction cascades (Thie *et al*., 1997, 1998). In RL95-2 cells, diltiazem-sensitive calcium channels enabled trophoblast binding, thus initiating cell binding, and SKF-96365-sensitive calcium channels participate in a feedback loop that controls the balance of bonds (Tinel *et al*., 2000). Certain integrin receptor complexes on the apical (free) aspect of these cells seem to play a major role in trophoblast adhesion to RL95-2 cells (Thie *et al*., 1995, 1996, 1997). Thus, this in-vitro model allows the study of complex signalling cascades and bond formation at the apical pole of uterine epithelial cells during trophoblast adhesion.

Although not yet studied in detail, small GTPases of the Rho family might represent one missing link in these signalling cascades. It is well known that Rho GTPases regulate various aspects of cell adhesion, including formation of focal contact sites and stress fibres (Bishop and Hall, 2000). Most importantly, Rho GTPases play an

essential role in membrane receptor signalling, including integrin receptors (Aplin *et al*., 1998). Rho proteins play a role in polarization of epithelial cells, i.e. the formation and organization of actin filaments, and in localization/function of actin-associated membrane proteins in the apex of these cells (Nusrat *et al*., 1995; Jou and Nelson, 1998). In addition, Rho GTPases have been shown to regulate morphological transition of epithelial cells to a fibroblastoid phenotype lacking epithelial-type polarity (Sander *et al*., 1999; Zondag *et al*., 2000). Thus, it was tempting to speculate that Rho GTPases might regulate properties of the apical pole of uterine epithelial cells that are crucial for adhesion competence for trophoblast binding.

Here, we studied the role of Rho GTPases in the regulation of adhesiveness of the apical pole of uterine epithelial RL95-2 cells for trophoblast-like JAR cells. We examined the expression of RhoA by high resolution fluorescence confocal microscopy, and its correlation with filamentous actin (F-actin) within the apex of RL95-2 cells. RhoA and F-actin were found to be tightly associated in the apex of uterine RL95-2 cells. RhoA distribution changed markedly when JAR cells attached at the apical pole of RL95-2 cells, and was associated with enhanced expression of F-actin at the binding sites. To examine the role of Rho GTPases in cell–cell adhesion, we used a specific inhibitor of Rho GTPases, *Clostridium difficile* toxin A, which glucosylates and thereby inactivates these GTPases, including RhoA (Just and Boquet, 2000). Using a functional adhesion assay, we found that Rho GTPases are necessary to establish cell–cell binding of uterine RL95-2 cells and JAR spheroids. In extrapolation to the in-vivo situation, these findings suggest that Rho protein signalling in human uterine epithelial cells plays an important role during the initial phase of embryo implantation, specifically in the context of trophoblast attachment and penetration.

Materials and methods

Reagents

The monoclonal mouse antibody 26CH:sc-418 to human RhoA was purchased from Santa Cruz Biotechnology (Heidelberg, Germany) and used in 1:50 dilution in phosphate-buffered saline (PBS) supplemented with 0.5% bovine serum albumin (BSA) for immunofluorescence, and in 1:1000 dilution in Tris-buffered saline supplemented with 0.1% BSA for Western blotting. The secondary antibody, Alexa Fluor 633-conjugated goat anti-mouse IgG (A-21052), was obtained from Molecular Probes (MoBiTec, Göttingen, Germany) and used in 1:150 dilution in PBS–BSA. To stain F-actin, a solution of tetramethylrhodamine isothiocyanate (TRITC)-conjugated phalloidin (Sigma–Aldrich, Deisenhofen, Germany) at a concentration of 25 µg/ml in PBS was used (Huang *et al*., 1992). For long-term tracing of JAR cells, a solution of the fluorescent dye, 5-chloromethylfluorescein diacetate (CMFDA) (Cell Tracker Green C-2925; Molecular Probes, MoBiTec, Göttingen, Germany), at a concentration of 1 µmol/ml in serum-free Roswell Park Memorial Institute (RPMI) 1640 medium (Gibco-Life Technology, Eggenstein, Germany) was used. UDP-[^{14}C]glucose (256 mCi/mmol) was obtained from Perkin–Elmer Life Sciences (Köln, Germany).

Cell culture

All cell lines were purchased from the American Type Culture Collection (ATCC; Rockville, MD, USA). The non-polar human uterine epithelial cell line RL95-2 (ATCC: CRL 1671) (Way *et al*., 1983) was maintained in a 1 + 1 mixture of Dulbecco's modified Eagle's medium (Gibco-Life Technology, Eggenstein, Germany) and Ham's F12 medium (Biochrom, Berlin, Germany), supplemented with 10% fetal calf serum (FCS) (Gibco), 10 mmol/l HEPES pH 7.4 (Biochrom), 5 µg/ml insulin (Sigma–Aldrich), 100 IU/ml penicillin (Boehringer, Mannheim, Germany) and 100 µg/ml streptomycin (Boehringer). The polar human uterine epithelial cell line HEC-1-A (ATCC: HTB 112) (Kuramoto *et al*., 1972) was maintained in McCoy's 5A medium (Biochrom) supplemented with 10% FCS, 100 IU/ml penicillin and 100 µg/ml streptomycin. For experiments, cells were cultured on poly-D-lysine-coated glass coverslips as described previously (John *et al*., 1993; Thie *et al*., 1995). As an invasive trophoblast model, multicellular spheroids of human choriocarcinoma JAR cells (ATCC: HTB 144) (Pattillo *et al*., 1971) were allowed to attach to the free surface of endometrial cell monolayers. JAR spheroids were prepared according to a published procedure (John *et al*., 1993), i.e. a suspension of 450 000 JAR cells per 6 ml RPMI 1640 medium (Gibco) supplemented with 10% FCS was agitated at 37°C on a gyratory shaker (Certomat R; Braun, Melsungen, Germany) at 110 rpm in order to form multicellular spheroids 72 h after initiation of culture.

Attachment of JAR speroids to RL95-2 cell monolayers

Details of the attachment assay have been described previously (John *et al*., 1993). In brief, JAR spheroids (see above) were harvested, counted, and gently delivered onto a confluent monolayer of endometrial RL95-2 cells grown on coverslips in JAR growth medium. After 60 min, spheroid adhesion to the endometrial monolayers was quantified by centrifugation of the coverslips with the cell-spheroid surface facing down at 12 *g* for 5 min. Attached spheroids were counted and expressed as a percentage of the number of seeded spheroids. In fluorescence confocal microscopy studies, attached JAR cells were distinguished from underlying endometrial cells by labelling of the JAR cells with the membrane-permeable fluorescent dye CMFDA, which after enzymatic cleavage serves as a long-term cytoplasmic marker. JAR spheroids were loaded with CMFDA for 45 min at 37°C, rinsed, incubated in growth medium without CMFDA for 30 min and delivered onto the free surface of endometrial monolayers as described above.

Clostridium difficile toxin A treatment

Endometrial RL95-2 cell monolayers were treated with purified *Clostridium difficile* toxin A (Chaves-Olarte *et al*., 1999) for the periods of time and toxin A concentrations as mentioned in the figure legends. Toxin A enters intact cells upon receptor-mediated endocytosis and monoglucosylates threonine 37/35 in endogenously expressed Rho GTPases (Just and Boquet, 2000). Immediately after toxin treatment, monolayers were processed to measure glucosylation of Rho GTPases in cell lysates in the presence of UDP-[^{14}C]glucose in-vitro or were used for cell–cell binding experiments (see above). [^{14}C]Glucosylation of endogenously expressed Rho GTPases in RL95-2 cell lysates was performed with 30 µmol/l UDP-[^{14}C]glucose (100 nCi) and 1 µg/ml toxin A as described previously (Schmidt *et al*., 1998).

Preparation of subcellular fractions and Western blotting

Subcellular fractions of endometrial cells were prepared essentially as described (Taguchi *et al*., 1998), with slight modifications. In brief, cells were washed with PBS, suspended in ice-cold buffer A (20 mmol/l Tris/HCl, pH 7.4, 2 mmol/l EDTA, 1 mmol/l EGTA, 1 mmol/l dithiothreitol, 1 mmol/l phenylmethylsulphonylfluoride, 50 µg/ml soybean trypsin inhibitor, 10 µmol/l pepstatin, 10 µmol/l leupeptin and 2 µg/ml aprotinin) and disrupted by three cycles of freeze–thawing, using liquid nitrogen and a 37°C water bath. This preparation (lysate) was then centrifuged at 17 000 *g* for 5 min, and the resulting supernatant was considered as the cytosolic fraction. The pellets were resuspended in ice-cold buffer A, supplemented with 1% Triton X-100, sonicated five times for 10 s each and centrifuged as above. The resulting supernatants were considered as the membrane fraction and the pellet as the cytoskeleton fraction. After boiling of the samples for 5 min in Laemmli buffer, proteins (per lane: lysate, 10 µg, cytosolic fraction and membrane as well as cytoskeleton, 100 µg each) were separated by sodium dodecyl sulphate–polyacrylamide gel electrophoresis on 12.5% acrylamide gels, transferred to nitrocellulose membranes, and stained with specific anti-RhoA antibodies (1 h incubation). The membranes were then incubated with secondary antibody, and immunoreactivity was visualized by enhanced chemiluminescence (Amersham Pharmacia Biotech, Freiburg, Germany) as described before (Schmidt *et al*., 1999).

F-actin staining

Samples were rinsed in PBS, fixed with 3% paraformaldehyde for 15 min at room temperature, permeabilized by incubation with 0.05% Triton X-100 for 2 min, and then incubated for 15 min with TRITC–phalloidin. After rinsing, the cells were mounted in PBS supplemented with 90% glycerol and 1.0% *p*-phenylenediamine and subsequently examined with the laser scanning microscope (see below).

Immunostaining

Samples were rinsed in PBS, fixed and permeabilized by a 1 + 1 mixture of ethanol–acetone for 10 min at room temperature. After four washing steps with PBS and after blocking non-specific binding sites by incubation with 0.5% BSA in PBS for 15 min, cells were incubated for 90 min at 37°C with the primary antibody (see above), which was omitted in control stainings. Thereafter, cells were rinsed in PBS/0.5% BSA and incubated with the corresponding fluorescence-conjugated secondary antibody (see above) for 90 min at 37°C. After rinsing, specimens were mounted in PBS supplemented with 90% glycerol and 1.0% *p*-phenylenediamine and subsequently examined with a laser scanning microscope. To combine immunofluorescence and F-actin staining, immunostaining was performed with the following modifications. Samples were not fixed and permeabilized in ethanol–acetone but fixed in paraformaldehyde and permeabilized in Triton X-100 according to the actin-staining protocol. Furthermore, the primary antibody and the TRITC–phalloidin were applied simultaneously, and both were omitted in controls. Thereafter, the immunostaining reaction was performed as described above.

Confocal laser scanning microsocopy

Confocal microsocopy was carried out using an Axiovert 100M microscope attached to a confocal laser scanning microscopy system (CLSM) (model LSM 510; Carl Zeiss, Jena, Germany) equipped with an argon laser (488 nm) and helium–neon lasers (543 and 633 nm respectively). Fluorescence emission of CMFDA was encoded as 'green' after passing a 505–530 nm bandpass filter, emission of TRITC as 'red' after passing a 560–565 nm bandpass filter, and emission of Alexa Fluor 633 as 'blue' after passing a 650 nm longpass filter. Image acquisition was done after optimizing CLSM settings with the range indicator palette. The pinhole size corresponded to a value of 1.0 of the airy disk as calculated by the CLSM software. Stacks of optical *xy*-sections at 0.5 µm intervals were collected with a 40-fold oil immersion objective with a numerical aperture of 1.30 NA. To reduce statistical noise, each optical slice was scanned eight times before being averaged.

Image analysis and processing

To obtain semi-quantitative data on cellular protein, the intensity of fluorescence was determined by measurement of grey scale values of each channel (Webb and Dorey, 1995) using the CLSM software (version 2.8 SR 1; Carl Zeiss, Jena, Germany). Image enhancement as well as calculation of colocalization coefficients (M_1 and M_2; Manders *et al*., 1993) and spatial measurements respectively, were performed with Image Pro Plus software (version 4.5; Media Cybernatics, Inc., Crofton, MD, USA) equipped with a Gaussian filter module (Adelmann, 1997) and a homomorphic filter plugin (Adelmann, 1998). Adobe Photoshop software (version 5.0; Adobe Systems Inc., San Jose, CA, USA) was used for arrangement of RGB-colour images out of single grey scale images each representing the signal of one colour channel. For three-dimensional reconstructions of samples, the Fortner T3D software (version 1.13; Research Systems, Inc., Boulder, CO, USA) was used after separating the colour channels from each stack of two-dimensional slices.

Statistical analysis

Mean values ± SE are presented with *n* denoting the number of experiments. The data were analysed both by using the Kruskal–Wallis test for global differences between groups and the Wilcoxon Signed Rank Sum test for their pairwise comparison. A value of $P < 0.05$ was considered significant.

Results

Subcellular localization of RhoA and F-actin in RL95-2 cells

As human uterine epithelial RL95-2 cells exhibit apical adhesiveness for trophoblast (John *et al*., 1993; Thie *et al*., 1995), we selected this cell type to study the role of Rho GTPases in trophoblast adhesion. First, we examined the subcellular localization of RhoA and its colocalization with F-actin, a major target of RhoA action, in monolayer cultured RL95-2 cells, using high resolution CLSM focusing on the apical (free) aspect of these cells. Maximal RhoA immunoreactivity was found in the cell periphery (Figure 1A, C). Although this pattern of staining was rather homogeneous, small RhoA-positive granules (diameter: 320 ± 60 nm; $n = 73$) could be detected, located preferentially in the apex of the cells (Figure 1D, F). No staining was observed in the nucleus. For comparison, F-actin was localized along the entire plasma membrane of the cells, forming a dense network which varied slightly in different cell regions (Figure 1B, C). Especially in the apical aspect of RL95-2 cells, small F-actin aggregates of irregular size were separated from each other by variable space (Figure 1E, F). Whether these aggregates might be equivalent to microvilli cores cannot be clarified unequivocally with CLSM alone. However, intact microvilli were rarely observed, which is in agreement with previous electron microscopic findings and consistent with the low degree of apico-basal polarity of RL95-2 cells (Thie *et al*., 1995, 1997).

Contact-induced changes of the subcellular localization of RhoA and F-actin

To monitor changes in RhoA and F-actin distribution initiated upon adhesion of trophoblast to RL95-2 cells, the latter were confronted with spheroids of trophoblast-like JAR cells (for illustration, see Figure 2). After 1 h of confrontation culture, RhoA distribution in the apical cell pole was no longer homogeneously fine-grained as in non-confronted RL95-2 cells (Figure 1), but rather coarsely grained (grain diameter: 820 ± 130 nm; $n = 73$) in the region of the JAR attachment site (Figure 3A, D). Similarly, F-actin distribution also changed, i.e. it was now condensed into big clumps embedded within a dense network of strong fibres beneath the cell membrane (Figure 3B, D).

Quantification of RhoA and F-actin fluorescence in the apex of RL95-2 cells revealed that JAR spheroid binding raised levels of RhoA fluorescence by ~2.8-fold and of F-actin fluorescence by ~4.8-fold, when compared with the levels found in the apex of non-confronted RL95-2 cells (Figure 4A). To measure the degree of overlap in fluorescence of RhoA and F-actin in RL95-2 cells, the colocalization coefficients were determined. At the apical aspect of non-confronted cells (Figure 1), 86.8% of RhoA staining was found to colocalize with F-actin staining and 51.3% of F-actin staining with RhoA (Figure 4B). These colocalization coefficients were altered in the apex of RL95-2 cells upon confrontation with JAR cells (Figure 3). RhoA now colocalized almost completely (97.9%) with F-actin, but only 43.8% of F-actin colocalized with RhoA (Figure 4B). This decrease in the F-actin colocalization coefficient probably reflects the drastic increase in the value of F-actin fluorescence within the plane of contact.

Three-dimensional reconstructions of confocal images provide a detailed view of the distribution of RhoA and F-actin staining in the apex of RL95-2 cells. In RL95-2 cells not confronted with spheroids of trophoblast-like JAR cells (Figure 5A, B), most of the RhoA is distributed homogeneously, but intermingled with small granules (Figure 5A), whereas F-actin appears in inhomogeneous large patches (Figure 5B). After apical binding of JAR cells (Figure 5C, D), RhoA domains are transformed into large clusters of organelles of a vesicular appearance (Figure 5C), while a massive, thickened F-actin network is formed at the same place in the apical submembrane region (Figure 5D).

Effect of toxin A on subcellular distribution of RhoA and F-actin in RL95-2 Cells

In order to study the role of Rho GTPases for adhesiveness of RL95-2 cells for JAR spheroids, RL95-2 cells were treated with *Clostridium difficile* toxin A, known to inactivate Rho family GTPases upon glucosylation of threonine 37/35 in the effector domain using cellular UDP-glucose as co-substrate (Just and Boquet, 2000). As

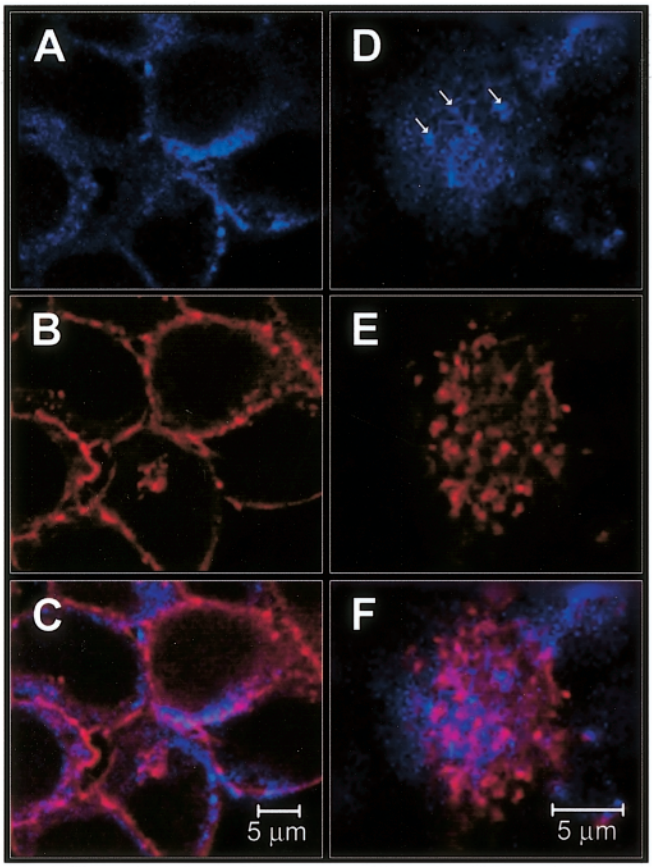

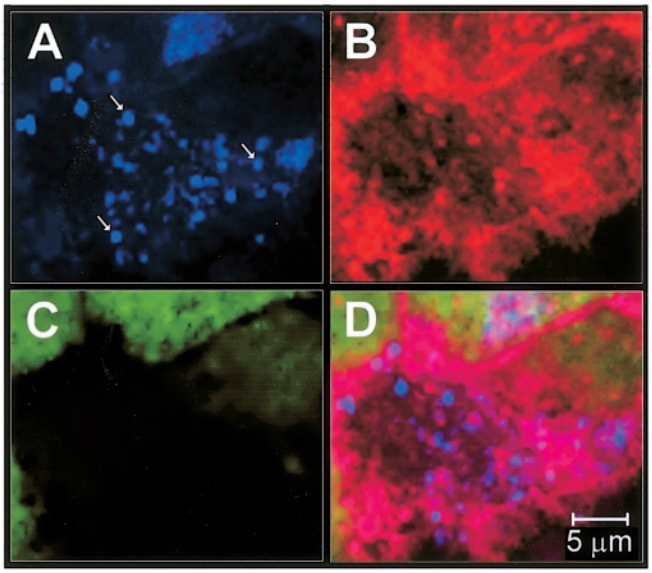

Figure 3

Figure 1

Figure 5

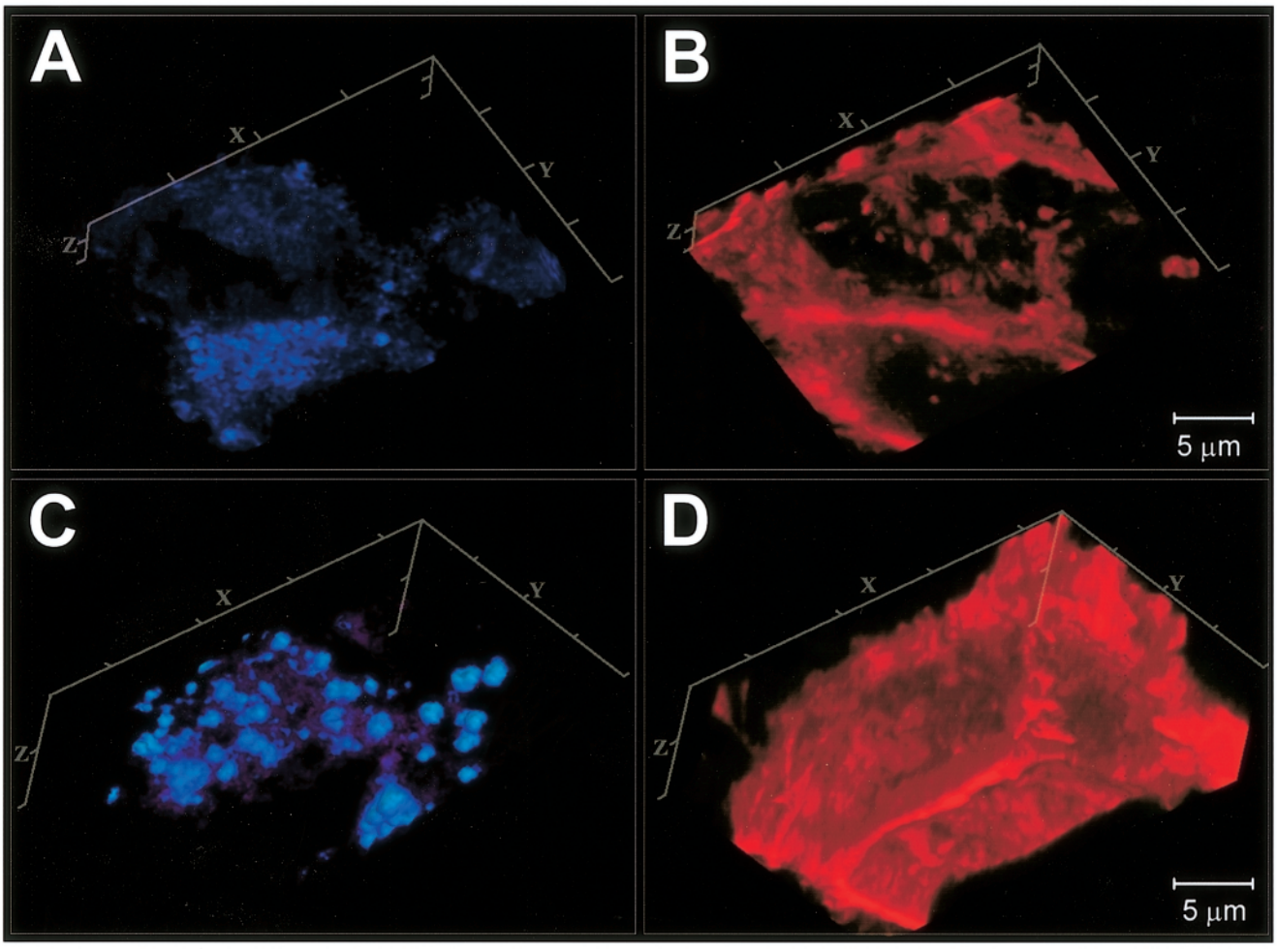

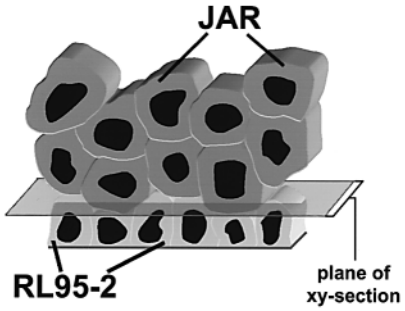

Figure 2. Three-dimensional sketch of a confrontation culture, showing a slice of the lower part of a multicellular JAR spheroid (JAR) and some of the monolayer-cultured RL95-2 cells (RL95-2) that are directly in contact. Due to the uneven surface of both spheroid and monolayer, contacts between JAR and RL95-2 cells are found at many sites. Note the plane of *xy*-section shown in Figure 3.

shown in Figure 6A, pretreatment of RL95-2 cells for 24 h with toxin A (1–500 ng/ml), in a concentration-dependent manner, reduced the toxin A-catalysed [^{14}C]glucosylation of Rho proteins, measured in lysates of the treated cells, indicating that toxin A treatment of the cells does in fact modify the endogenous Rho proteins. Treatment of RL95-2 cells with toxin A (100 ng/ml for 24 h) drastically altered the subcellular distribution of RhoA, as examined by Western blot analysis of subcellular fractions with a specific anti-RhoA antibody (Figure 6B). In line with the confocal microscopy data, in untreated RL95-2 cells RhoA was found mainly in the membrane fraction, while only small amounts of RhoA were detected in the cytosolic and cytoskeleton fractions. On the other hand, RhoA was equally distributed between the membrane and cytosolic fractions of HEC-1-A cell monolayers, a well-polarized human uterine epithelial cell line (Figure 6C). After toxin A treatment of RL95-2 cells, the amount of RhoA in the membrane fraction was strongly reduced, with comparable increases in the cytosolic and cytoskeleton fractions. Although toxin A induced such a dramatic switch in the subcellular localization of RhoA in RL95-2 cells, the overall expression level of RhoA was not changed (Figure 6B). Quantification of RhoA and F-actin fluorescence in the apical aspect of toxin A-treated RL95-2 exhibited reductions to 84 and 62% respectively, when compared with untreated cells (Figure 7A). Probably as a result of this change, the values of the colocalization coefficients of RhoA and F-actin were altered, i.e. 54.8% of RhoA colocalized with F-actin and 68.3% of F-actin colocalized with RhoA (Figure 7B).

Loss of cell–cell binding upon Rho protein inactivation

When cultured as confluent monolayers, RL95-2 cells showed adhesive properties for trophoblast-like JAR cells. After 1 h of confrontation culture, JAR spheroids showed high values of attachment (72.9%) to RL95-2 cells, compared with poly-D-lysine coated glass coverslips (39.0%) used as controls (Figure 8). These data are similar to previously published results obtained with this

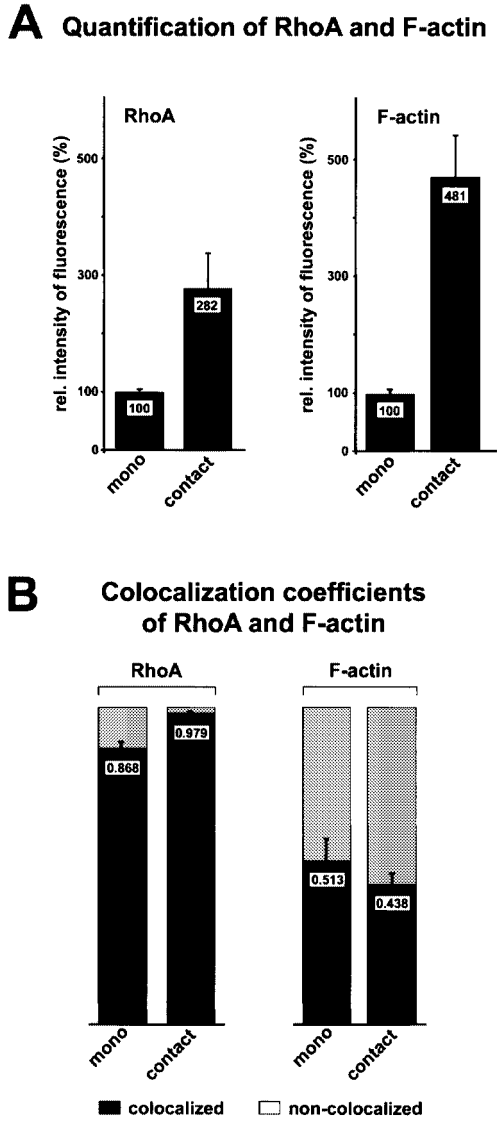

Figure 4. (**A**) Quantification of RhoA and F-actin in the apex of monolayer cultured RL95-2 cells before (mono) and after binding of JAR spheroids (contact). For semi-quantitative evaluation of fluorescence, grey values of each colour channel were determined within double-labelled cells. Stacks of 6 *xy*-sections at 0.5 μm intervals were collected with the first marked slice at the apical cell surface. Numbers of RL95-2 cells tested: $n = 9$ (mono), $n = 7$ (contact). (**B**) Colocalization coefficients of RhoA colocalizing with F-actin and F-actin colocalizing with RhoA in the apex of RL95-2 cells before (mono) and after binding of JAR spheroids (contact). Numbers of RL95-2 cells tested: $n = 13$ (mono), $n = 6$ (contact). Values are mean ± SE. The differences between groups before and after spheroid binding are statistically significant ($P < 0.05$).

Figure 1. Localization of RhoA (**A**, **D**) (blue) and F-actin (**B**, **E**) (red) in the apical pole of RL95-2 monolayers. *xy*-sections are from the upper third of cells (**A**–**C**), or are grazing the apical plasma membrane (**D**–**F**). Merger of the confocal images (**C**, **F**). Typical patterns are presented. Arrows (**D**) indicate RhoA granules.

Figure 3. Localization of RhoA (**A**) (blue) and F-actin (**B**) (red) in an *xy*-section of a confrontation culture, focusing on the plane of RL95-2/JAR spheroid contact. Staining of JAR cells with CMFDA (green) (**C**). Merger of these confocal images is shown in (**D**). Typical patterns are presented. Note the big vesicles of RhoA (indicated by arrows in **A**) and extended clumps of F-actin.

Figure 5. View from the cytoplasmic side of an RL95-2 cell showing the submembraneous RhoA distribution (**A**, **C**) (blue) and F-actin organization (**B**, **D**) (red) at the apical cell pole before (**A**, **B**) and after (**C**, **D**) binding of JAR spheroids. Images **A** and **B** and images **C** and **D** respectively, are derived from the same cell after separating the colour channels from each stack of optical *xy*-sections. Three-dimensional rendering was obtained upon rotation of the reconstructions. Note the appearance of large RhoA vesicles (**C**) and the increase of F-actin (**D**) along the cytoplasmic surface of the apex of RL95-2 cells upon JAR binding.

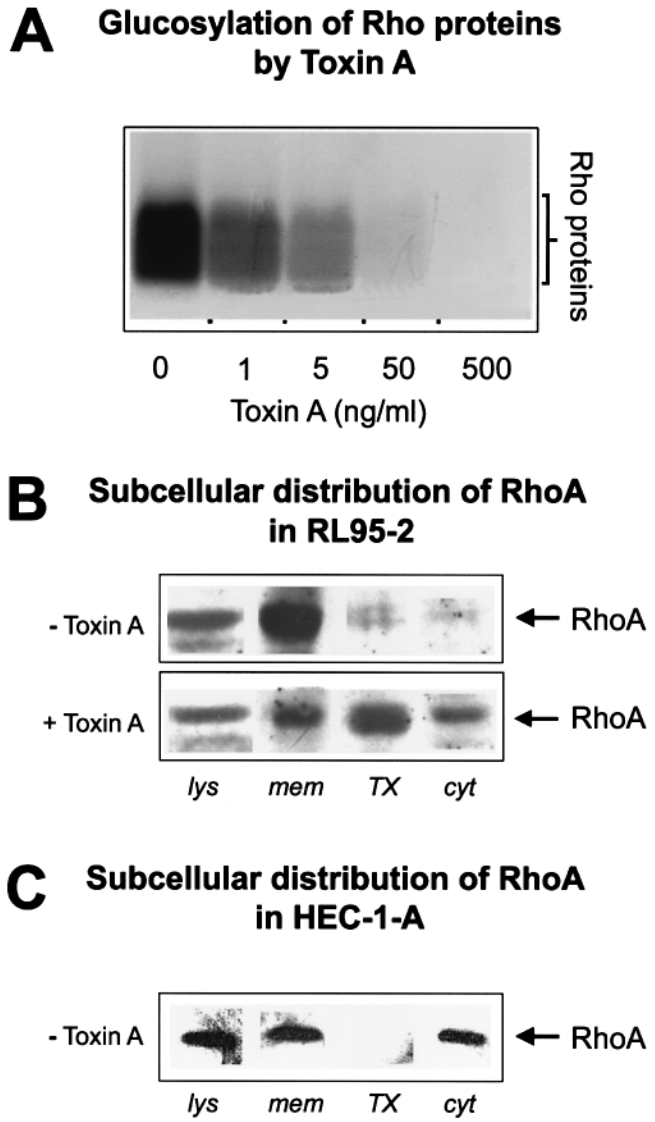

Figure 6. (**A**) Glucosylation of endogenous Rho GTPases by toxin A in RL95-2 cells. Toxin A-catalysed [^{14}C]glucosylation was determined in lysates of cells treated for 24 h without (0) and with the indicated toxin A concentrations. The autoradiogram of the SDS–PAGE is shown. The toxin A substrates were identified as Rho GTPases by immunoblotting (data not shown). (**B**) Immunoblot analysis of endogenously expressed RhoA in RL95-2 monolayers treated without (– Toxin A) and with 100 ng/ml toxin A for 24 h (+ Toxin A). (**C**) For comparison, immunoblot analysis of RhoA in untreated HEC-1-A cells is shown. Preparation of cell lysates (*lys*), membranes (*mem*), cytoskeleton fraction (*TX*) and cytosol (*cyt*) of cells was performed as described. Proteins (lysates: 10 µg/lane; membranes, cytoskeleton fraction, cytosol: each 100 µg/lane) were separated by SDS–PAGE and subsequently immunoblotted. Data shown are typical for three to five independent experiments.

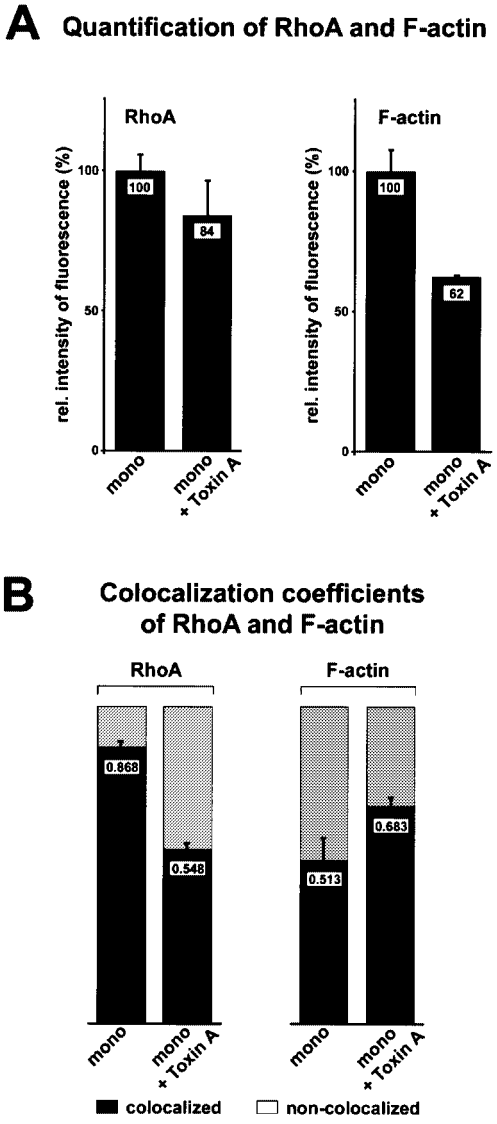

Figure 7. (**A**) Quantification of RhoA and F-actin in the apex of monolayer cultured RL95-2 cells before (mono) and after treatment with 100 ng/ml toxin A for 24 h (mono + Toxin A). For semi-quantitative evaluation of fluorescence, grey values of each colour channel were determined within double-labelled cells. Stacks of six *xy*-sections at 0.5 µm intervals were collected with the first marked slice at the apical cell surface. Numbers of RL95-2 cells tested: $n = 9$ (mono), $n = 15$ (mono + Toxin A). (**B**) Colocalization coefficients of RhoA colocalizing with F-actin and F-actin colocalizing with RhoA in the apex of RL95-2 cells before (mono) and after treatment with toxin A (mono + Toxin A). Numbers of cells: $n = 13$ (mono), $n = 14$ (mono + Toxin A). Values are mean ± SE. The differences between groups before and after toxin A treatment are all statistically significant ($P < 0.05$).

attachment assay (John *et al*., 1993; Thie *et al*., 1995). Treatment of RL95-2 cells with toxin A (100 ng/ml for 24 h) did not alter the morphology of monolayer-cultured cells (data not shown). However, such treatment with toxin A suppressed the trophoblast-adhesive properties of RL95-2 cells (Figure 8). After toxin A treatment of RL95-2 cells, JAR cells showed values of attachment (43.4%) comparable with those of attachment to glass coverslips without RL95-2 cells. Thus, adhesiveness of RL95-2 cells for trophoblast-like JAR cells, a characteristic not found in the polar uterine epithelial cell line HEC-1-A (John *et al*., 1993; Thie *et al*., 1995), was lost upon inactivation of Rho proteins.

Discussion

The mechanisms regulating the adhesiveness of the uterine epithelium to trophoblast during initiation of human embryo implantation are incompletely understood. Using monolayer-cultured endometrial RL95-2 cells as an in-vitro model for the human receptive uterine epithelium (John *et al*., 1993; Thie *et al*., 1996, 1997, 1998), we demonstrate here that formation of stable cell–cell binding between uterine epithelial RL95-2 cells and spheroids of trophoblast-like JAR cells depends on Rho GTPases, most likely RhoA. Furthermore, our data imply that remodelling of the actin cytoskeleton in the presence of RhoA in the apical submembrane region of uterine epithelial cells is directly involved in trophoblast binding.

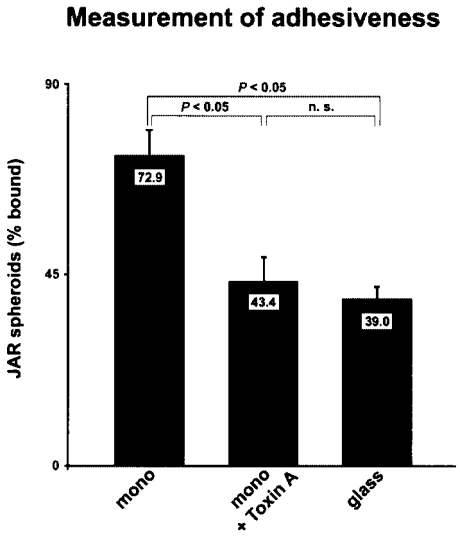

Figure 8. Effect of toxin A on adhesiveness of RL95-2 cells for JAR spheroids. Monolayer cultured RL95-2 cells were treated for 24 h without (mono) and with 100 ng/ml toxin A (mono + Toxin A). Thereafter, adhesion of JAR spheroids to RL95-2 cells was determined as described. For comparison, adhesion of JAR spheroids to poly-D-lysine-coated glass coverslips (glass) is shown. Adhesion is expressed as the percentage of the number of spheroids seeded. Number of spheroids: $n = 1096$ (mono), $n = 1115$ (mono + Toxin A), $n = 1029$ (glass). Values are mean ± SE. n.s. = not significant.

As shown previously, confrontation of RL95-2 cells via their free pole with the trophoblast-like JAR cells results in the formation of cell–cell adhesion sites (Thie *et al*., 1998). Moreover, cytoskeletal perturbation by cytochalasin D decreases adhesive properties of the apical pole of RL95-2 cells, indicating that an unaltered organization of the actin cytoskeleton is indispensable for JAR spheroid adhesion (Thie *et al*., 1997). Interestingly, as shown here, trophoblast binding led not only to a marked increase of F-actin at the newly formed binding sites in the apex of RL95-2 cells, but likewise also to an increase of colocalized RhoA. These results indicate that RL95-2 cells respond to JAR cell contact with an alteration of F-actin distribution in these apical cell–cell adhesion sites and with a subcellular redistribution of RhoA. Likewise, it has been demonstrated that activation of epithelial MDCK cells by hepatocyte growth factor induces translocation of RhoA from the cytoplasm to the membrane ruffling area, cell–cell adhesion sites and cleavage furrows (Takaishi *et al*., 1995). Most interestingly, inhibition of Rho-dependent signalling in uterine RL95-2 cells upon treatment with *Clostridium difficile* toxin A inhibited binding of trophoblastic cells. Furthermore, toxin A treatment reduced RhoA colocalization with F-actin within the apex of RL95-2 cells, and strongly reduced the proportion of RhoA in the membrane fraction of the cells. On the other hand, in NIH-3T3 fibroblasts, inactivation of RhoA by *Clostridium difficile* toxin A blocks its cytosol–membrane cycling and increases the amount of membrane-associated RhoA (Genth *et al*., 1999). RL95-2 cells represent an epithelium-derived cell line (Thie *et al*., 1996), and this difference in cell type probably explains the different effects of toxin A on the subcellular distribution of RhoA in NIH-3T3 fibroblasts versus RL95-2 cells. Furthermore, HEC-1-A cells, a well-polarized uterine epithelial cell type, differ not only in their cell morphology (Thie *et al*., 1995) but also in their subcellular distribution of RhoA from RL95-2 cells insofar as RhoA was found equally distributed between the membrane and cytosolic fractions. Taken together, we have demonstrated here that inactivation of Rho GTPases by toxin A induces, in human uterine epithelial cells, alterations in the subcellular localization of RhoA and a dramatically altered competence for trophoblast binding. As inactivation of Rho proteins by toxin A prevents their interaction with effector proteins (Pothoulakis, 2000; Schmitz *et al*., 2000), such effector proteins are probably essential mediators of RhoA-dependent apical cell–cell binding between RL95-2 cells and JAR spheroids.

The molecules that mediate trophoblast adhesion to uterine epithelial cells are not well defined. Possible candidates are trophinin (Aoki and Fukuda, 2000), cadherins (Thie *et al*., 1995) and integrins (Albers *et al*., 1995; Lessey *et al*., 1995; Thie *et al*., 1995, 1997; Lessey, 1998). In addition, anti-adhesion systems may regulate the first steps of this cell–cell interaction (Chervenak and Illsley, 2000; Meseguer *et al*., 2001). Interestingly, increased adhesiveness of RL95-2 cells is associated with down-regulation or absence of moesin (Martin *et al*., 2000), known to regulate cell–matrix contacts and cell–cell contacts in other systems (Geiger *et al*., 2001). We have shown before that adhesiveness of RL95-2 cells for trophoblast requires integrin receptor signalling (Thie *et al*., 1995, 1996, 1997). This is of particular interest, since it is well established that Rho GTPases play a major role in outside-in signalling by integrins (Aplin *et al*., 1998; Schwartz and Shattil, 2000). As activation of Rho proteins by calcium influx has been reported (Masiero *et al*., 1999) and as calcium influx in RL95-2 cells is connected with binding of JAR cells (Tinel *et al*., 2000), it is tempting to speculate that calcium and integrin receptor signalling may converge on the level of RhoA to trigger the required cytoskeletal changes. Reorganization of the actin cytoskeleton by activated RhoA is mediated by RhoA effector proteins, most notably the Rho-associated Rho-kinase and the phosphatidylinositol-4-phosphate 5-kinase, both of which are known to regulate the organization of the actin cytoskeleton (Aplin *et al*., 1998; Hemler, 1998; Schmidt *et al*., 1999; Oude Weernink *et al*., 2000; Schmitz *et al*., 2000; Schwartz and Shattil, 2000; Geiger and Bershadsky, 2001; Noren *et al*., 2001). Beside Rho GTPases, integrin receptors are known to activate Ras and Ras-like GTPases, such as Rap2B, which play important roles in receptor signalling in diverse cell types (Aplin *et al*., 1998; Schmidt *et al*., 2001). Thus, other members of the small GTPase superfamily may also be involved in the process of trophoblast binding and adhesion to RL95-2 cells; however, this was beyond the scope of the present study. Furthermore, Rho GTPases are probably of functional importance also for other aspects of the implantation cascade and not only for the initial steps of adhesion between uterine epithelial cells and trophoblast. As recently reported (Shiokawa *et al*., 2000), RhoA also plays an essential role in decidual cells for embryonic development and differentiation, suggesting that Rho GTPases control several aspects of embryo implantation.

Changes in the subcellular localization of Rho proteins are part of complex morphological and cell biological transformations that uterine epithelial cells undergo during the receptive period, i.e. in preparation for the implantation process. Various observations suggest that the blastocyst can only overcome the uterine epithelium barrier when the luminal epithelial cells have switched from a non-receptive to a receptive state (Bentin-Ley *et al*., 2000; Carson *et al*., 2000; Kimber and Spanswick, 2000; Denker and Thie, 2001). The receptive state may be under the control of master genes, which prepare the apical cell pole of uterine cells for contact with the trophoblast upon down-regulation of the polarized cytoplasmic organization (Denker, 1993, 1994). For example, changes include reorganization of the actin cytoskeleton (Murphy, 1995, 2000a,b) and the intermediate filament system (Hochfeld *et al*., 1990). RL95-2 cells used as a model in the present investigation stably express a phenotype of uterine epithelial cells that lack a pronounced apico-basal axis (Thie *et al*., 1995) as well as any tight junctions, and that have only a primitive type of adherens junction and cytoskeletal organization (Thie *et al*., 1996, 1997). These characteristics are obviously relevant for the

adhesiveness of their free cell pole for trophoblast, as uterine epithelial HEC-1-A cells, which exhibit a well-developed epithelial polarity (Drubin and Nelson, 1996; Yeaman *et al*., 1999), do not allow trophoblast to adhere (John *et al*., 1993; Thie *et al*., 1995). Rho proteins have been reported to be required to establish a fully polarized state as well as a non-polarized phenotype upon epithelial-to-mesenchymal transition (Nusrat *et al*., 1995; Jou and Nelson, 1998; Sander *et al*., 1999; Schmitz *et al*., 2000; Zondag *et al*., 2000), although the exact role of Rho proteins in these processes remains to be determined (Price and Collard, 2001). The high degree of colocalization of RhoA with F-actin in the apex of RL95-2 cells even in non-confrontation cultures, i.e. under unstimulated conditions, is consistent with the view that RL95-2 cells are an intermediate between a well-polarized and non-polarized phenotype. In order to exhibit adhesion competence for trophoblast, uterine epithelial cells apparently need to express an epithelial (not a mesenchymal) phenotype but with reduced or destabilized apico-basal polarity (Denker, 1993, 1994).

In conclusion, our data are consistent with the concept that uterine epithelial cells in the receptive state possess a cytoplasmic/membrane architecture of a modified type with reduced/down-regulated apico-basal polarity and an apical cell pole which is equipped with appropriate sets of adhesion molecules. In addition, an increasing amount of data suggests that, in conjunction with trophoblast binding, a cascade of signalling events must be initiated in the apical submembrane region of uterine epithelial cells. These events, which require Rho GTPases, most likely RhoA, are indeed an essential element of adhesion of trophoblast and of embryo implantation initiation.

Acknowledgements

We thank Dr H.G.Adelmann for constructive criticisms in advanced digital image processing and for kind provision of his Gauss bandpass and homomorphic filter plugins, Dr J.Hüsing for help with statistical analysis and Dr C.von Eichel-Streiber for providing toxin A. The skilful technical assistance of K.Baden, B.Gobs, B.Maranca and D.Schünke is gratefully acknowledged. This work was supported by the Deutsche Forschungsgemeinschaft (DFG) and the Interne Forschungsförderung Essen (IFORES).

References

Adelmann, H.G. (1997) A frequency-domain Gaussian filter module for quantitative and reproducible high-pass, low-pass and band-pass filtering of images. *Am. Lab*., **29**, 27–33.

Adelmann, H.G. (1998) Butterworth equations for homomorphic filtering of images. *Comput. Biol. Med*., **28**, 169.

Albers, A., Thie, M., Hohn, H.P. and Denker, H.-W. (1995) Differential expression and localization of integrins and CD44 in the membrane domains of human uterine epithelial cells during the menstrual cycle. *Acta Anat*., **153**, 12–19.

Aoki, R. and Fukuda, M.N. (2000) Recent molecular approaches to elucidate the mechanism of embryo implantation: trophinin, bystin, and tastin as molecules involved in the initial attachment of blastocysts to the uterus in humans. *Semin. Reprod. Med*., **18**, 265–271.

Aplin, A.E., Howe, A., Alahari, S.K. and Juliano, R.L. (1998) Signal transduction and signal modulation by cell adhesion receptors: the role of integrins, cadherins, immunoglobulin-cell adhesion molecules, and selectins. *Pharmacol. Rev*., **50**, 197–263.

Armant, D.R., Wang, J. and Liu, Z. (2000) Intracellular signaling in the developing blastocyst as a consequence of the maternal–embryonic dialogue. *Semin. Reprod. Med*., **18**, 273–287.

Bentin-Ley, U., Horn, T., Sjögren, A., Sörensen, S., Falck Larsen, J. and Hamberger, L. (2000) Ultrastructure of human blastocyst–endometrial interactions in vitro. *J. Reprod. Fertil*., **120**, 337–350.

Bishop, A.L. and Hall, A. (2000) Rho GTPases and their effector proteins. *Biochem. J*., **348**, 241–255.

Carson, D.D., Bagchi, I., Dey, S.K., Enders, A.C., Fazleabas, A.T., Lessey, B.A. and Yoshinaga, K. (2000) Embryo implantation. *Dev. Biol*., **223**, 217–237.

Chaves-Orlate, E., Löw, P., Freer, E., Norlin, T., Weidmann, M., von Eichel-Streiber, C. and Thelestam, M. (1999) A novel cytotoxin from *Clostridium difficile* serogroup F is a functional hybrid between two other large clostridial cytotoxins. *J. Biol. Chem*., **274**, 11046–11052.

Chervenak, J.L. and Illsley, N.P. (2000) Episialin acts as an antiadhesive factor in an in vitro model of human endometrial-blastocyst attachment. *Biol. Reprod*., **63**, 294–300.

Denker, H.-W. (1993) Implantation: a cell biological paradox. *J. Exp. Zool*., **266**, 541–558.

Denker, H.-W. (1994) Endometrial receptivity: cell biological aspects of an unusual epithelium. *Ann. Anat*., **176**, 53–60.

Denker, H.-W. and Thie, M. (2001) The regulatory function of the uterine epithelium for trophoblast attachment: experimental approaches. *Int. J. Anat. Embryol*., **106** (Suppl. 2), 291–306.

Drubin, D.G. and Nelson, W.J. (1996) Origins of cell polarity. *Cell*, **84**, 335–344.

Geiger, B. and Bershadsky, A. (2001) Assembly and mechanosensory function of focal contacts. *Curr. Opin. Cell Biol*., **13**, 584–592.

Geiger, B., Bershadsky, A., Pankov, R. and Yamada, K.M. (2001) Transmembrane crosstalk between the extracellular matrix–cytoskeleton crosstalk. *Nat. Rev. Mol. Cell Biol*., **2**, 793–805.

Genth, H., Aktories, K. and Just, I. (1999) Monoglucosylation of RhoA at threonine 37 blocks cytosol–membrane cycling. *J. Biol. Chem*., **274**, 29050–29056.

Hemler, M.E. (1998) Integrin associated proteins. *Curr. Opin. Cell Biol*., **10**, 578–585.

Hochfeld, A., Beier, H.M. and Denker, H.-W. (1990) Changes of intermediate filament protein localization in endometrial cells during early pregnancy of rabbits. In Denker, H.-W. and Aplin, J.D. (eds), *Trophoblast Invasion and Endometrial Receptivity. Novel Aspects of the Cell Biology of Embryo Implantation. Trophoblast Research*, Vol. 4. Plenum, New York, pp. 357–374.

Hohn, H.P., Linke, M. and Denker, H.-W. (2000) Adhesion of trophoblast to uterine epithelium as related to the state of trophoblast differentiation: in vitro studies using cell lines. *Mol. Reprod. Dev*., **57**, 135–145.

Huang, Z., Haugland, R.P., You, W. and Haugland, R.P. (1992) Phallotoxin and actin binding assay by fluorescence enhancement. *Anal. Biochem*., **200**, 199–204.

John, N.J., Linke, M. and Denker, H.-W. (1993) Quantitation of human choriocarcinoma spheroid attachment to uterine epithelial cell monolayers. *In Vitro Cell. Dev. Biol*., **29A**, 461–468.

Jou, T.-S. and Nelson, W.J. (1998) Effects of regulated expression of mutant RhoA and Rac1 small GTPases on the development of epithelial (MDCK) cell polarity. *J. Cell Biol*., **142**, 85–100.

Just, I. and Boquet, P. (2000) Large clostridial cytotoxins as tools in cell biology. *Curr. Top. Microbiol. Immunol*., **250**, 97–107.

Kimber, S.J. and Spanswick, C. (2000) Blastocyst implantation: the adhesion cascade. *Semin. Cell Dev. Biol*., **11**, 77–92.

Kuramoto, H., Tamura, S. and Notake, Y. (1972) Establishment of a cell line of human endometrial adenocarcinoma *in vitro*. *Am. J. Obstet. Gynecol*., **114**, 1012–1019.

Lessey, B.A. (1998) Endometrial integrins and the establishment of uterine receptivity. *Hum. Reprod*., **13**, 247–258.

Lessey, B.A., Castelbaum, A.J., Sawin, S.W. and Sun, J. (1995) Integrins as markers of uterine receptivity in women with primary unexplained infertility. *Fertil. Steril*., **63**, 535–542.

Liu, S., Julian, J. and Carson, D.D. (1998) A peptide sequence of heparin/heparan sulfate (HP/HS)-interacting protein supports selective, high affinity binding of HP/HS and cell attachment. *J. Biol. Chem*., **273**, 9718–9726.

Manders, E.M.M., Verbeek, F.J. and Aten, J.A. (1993) Measurement of co-localization of objects in dual-colour confocal images. *J. Microsc*., **169**, 375–382.

Martin, J.C., Jasper, M.J., Valbuena, D., Meseguer, M., Remohi, J., Pellicer, A. and Simon, C. (2000) Increased adhesiveness in cultured endometrial-derived cells is related to the absence of moesin expression. *Biol. Reprod*., **63**, 1370–1376.

Masiero, L., Lapidos, K.A., Ambudkar, I. and Kohn, E.C. (1999) Regulation of the RhoA pathway in human endothelial cell spreading on type IV collagen: role of calcium influx. *J. Cell Sci*., **112**, 3205–3213.

Meseguer, M., Aplin, J.D., Caballero-Campo, P., O'Connor, J.E., Martin, J.C., Remohi, J., Pellicer, A. and Simon, C. (2001) Human endometrial mucin MUC1 is up-regulated by progesterone and down-regulated in vitro by the human blastocyst. *Biol. Reprod*., **64**, 590–601.

Murphy, C.R. (1995) The cytoskeleton of uterine epithelial cells: a new player in uterine receptivity and the plasma membrane transformation. *Hum. Reprod. Update*, **1**, 567–580.

Murphy, C.R. (2000a) The plasma membrane transformation of uterine epithelial cells during pregnancy. *J. Reprod. Fertil.*, **55** (Suppl.), 23–28.

Murphy, C.R. (2000b) Junctional barrier complexes undergo major alterations during the plasma membrane transformations of uterine epithelial cells. *Hum. Reprod.*, **15** (Suppl. 3), 182–188.

Nikas, G. (1999) Cell-surface morphological events relevant to human implantation. *Hum. Reprod.*, **14** (Suppl. 2), 37–44.

Noren, N.K., Niessen, C.M., Gumbiner, B.M. and Burridge, K. (2001) Cadherin engagement regulates Rho family GTPases. *J. Biol. Chem.*, **276**, 33305–33308.

Nusrat, A., Giry, M., Turner, J.R., Colgan, S.P., Parkos, C.A., Carnes, D., Lemichez, E., Boquet, P. and Madara, J.L. (1995) Rho protein regulates tight junctions and perijunctional actin organization in polarized epithelia. *Proc. Natl. Acad. Sci. USA*, **92**, 10629–10633.

Oude Weernink, P.A., Schulte, P., Guo, Y., Wetzel, J., Amano, M., Kaibuchi, K., Haverland, S., Voss, M., Schmidt, M., Mayr, G.M. and Jakobs, K.H. (2000) Stimulation of phosphatidylinositol-4-phosphate 5-kinase by Rho-kinase. *J. Biol. Chem.* **275**, 10168–10174.

Pattillo, R.A., Ruckert, A., Hussa, R., Bernstein, R. and Delfs, E. (1971) The JAR cell line—continuous human multihormone production and controls. *In Vitro*, **6**, 398.

Perret, S., Dockery, P. and Harvey, B.J. (2001) 17β-Oestradiol stimulates capacitative Ca^{2+} entry in human endometrial cells. *Mol. Cell. Endocrinol.*, **176**, 77–84.

Pothoulakis, C. (2000) Effects of *Clostridium difficile* toxins on epithelial cell barrier. *Ann. NY Acad. Sci.*, **915**, 347–356.

Price, L.S. and Collard, J.G. (2001) Regulation of the cytoskeleton by Rho-family GTPases: implications for tumour cell invasion. *Semin. Cancer Biol.*, **11**, 167–173.

Raboudi, N., Julian, J., Rohde, L.H. and Carson, D.D. (1992) Identification of cell surface heparin/heparan sulfate binding proteins of a human uterine epithelial cell line (RL95). *J. Biol. Chem.*, **267**, 11930–11939.

Rhode, L.H. and Carson, D.D. (1993) Heparin-like glycosaminoglycans participate in binding of a human trophoblastic cell line (JAR) to a human uterine epithelial cell line (RL95). *J. Cell. Physiol.*, **155**, 185–196.

Sander, E.E., ten Klooster, J.P., van Delft, S., van der Kammen, R.A. and Collard, J.G. (1999) Rac downregulates Rho activity: reciprocal balance between both GTPases determines cellular morphology and migratory behavior. *J. Cell Biol.*, **147**, 1009–1021.

Schmidt, M., Voβ, M., Thiel, M., Bauer, B., Grannass, A., Tapp, E., Cool, R.H., de Gunzburg, J., von Eichel-Streiber, C. and Jakobs, K.H. (1998) Specific inhibition of phorbol ester-stimulated phospholipase D by *Clostridium sordellii* lethal toxin and *Clostridium difficile* toxin B-1470 in HEK-293 cells. Restoration by Ral GTPases. *J. Biol. Chem.*, **273**, 7413–7422.

Schmidt, M., Voβ, M., Oude Weernink, P.A., Wetzel, J., Amano, M., Kaibuchi, K. and Jakobs, K.H. (1999) A role for Rho-kinase in Rho-controlled phospholipase D stimulation by the m3 muscarinic acetylcholine receptor. *J. Biol. Chem.* **274**, 14648–14654.

Schmidt, M., Evellin, S., Oude Weernink, P.A., van Dorp, F., Rehmann, H., Lomasney, J.W. and Jakobs, K.H. (2001) A new phospholipase–C-calcium signalling pathway mediated by cyclic AMP and a Rap GTPase. *Nat. Cell Biol.* **3**, 1020–1024.

Schmitz, A.A.P., Govek, E.-E., Böttner, B. and Van Aelst, L. (2000) Rho GTPases: signaling, migration and invasion. *Exp. Cell Res.*, **261**, 1–12.

Schwartz, M.A. and Shattil, S.J. (2000) Signaling networks linking integrins and Rho family GTPases. *Trends Biochem. Sci.*, **25**, 388–391.

Shiokawa, S., Sakai, K., Akimoto, Y., Suzuki, N., Hanashi, H., Nagamatsu, S., Iwashita, M., Nakamura, Y., Hirano, H. and Yoshimura, Y. (2000) Function of the small guanosine triphosphate-binding protein RhoA in the process of implantation. *J. Clin. Endocrinol. Metab.*, **85**, 4742–4749.

Taguchi, K., Yang, M., Goepel, M. and Michel, M.C. (1998) Comparison of human α_1-adrenoceptor subtype coupling to protein kinase C activation and related signalling pathways. *Naunyn-Schmiedeberg's Arch. Pharmacol.*, **357**, 100–110.

Takaishi, K., Sasaki, T., Kameyama, T., Tsukita, S., Tsukita, S. and Takai, Y. (1995) Translocation of activated Rho from the cytoplasm to membrane ruffling area, cell–cell adhesion sites and cleavage furrows. *Oncogene*, **11**, 39–48.

Thie, M., Harrach-Ruprecht, B., Sauer, H., Fuchs, P., Albers, A. and Denker, H.-W. (1995) Cell adhesion to the apical pole of epithelium: a function of cell polarity. *Eur. J. Cell Biol.*, **66**, 180–191.

Thie, M., Fuchs, P., Butz, S., Sieckmann, F., Hoschützky, H., Kemler, R. and Denker, H.-W. (1996) Adhesiveness of the apical surface of uterine epithelial cells: the role of junctional complex integrity. *Eur. J. Cell Biol.*, **70**, 221–232.

Thie, M., Herter, P., Pommerenke, H., Dürr, F., Sieckmann, F., Nebe, B., Rychly, J. and Denker, H.-W. (1997) Adhesiveness of the free surface of a human endometrial monolayer for trophoblast as related to actin cytoskeleton. *Mol. Hum. Reprod.*, **3**, 275–283.

Thie, M., Röspel, R., Dettmann, W., Benoit, M., Ludwig, M., Gaub, H.E. and Denker, H.-W. (1998) Interaction between trophoblast and uterine epithelium: monitoring of adhesive forces. *Hum. Reprod.*, **13**, 3211–3219.

Tinel, H., Denker, H.-W. and Thie, M. (2000) Calcium influx in human uterine epithelial RL95-2 cells triggers adhesiveness for trophoblast-like cells. Model studies on signalling events during embryo implantation. *Mol. Hum. Reprod.*, **6**, 1119–1130.

Way, D.L., Grosso, D.S., Davis, J.R., Surwit, E.A. and Christian, C.D. (1983) Characterization of a new human endometrial carcinoma (RL95-2) established in tissue culture. *In Vitro*, **19**, 147–158.

Webb, R.H. and Dorey, C.K. (1995) The pixilated image. In Pawley, J.B. (ed.), *Handbook of Biological Confocal Microscopy*, 2nd edn. Plenum Press, New York, pp. 55–67.

Yeaman, C., Grindstaff, K.K. and Nelson, W.J. (1999) New perspectives on mechanisms involved in generating epithelial cell polarity. *Physiol. Rev.*,**79**, 73–98.

Zondag, G.C.M., Evers, E.E., ten Klooster, J.P., Janssen, L., van der Kammen, R.A. and Collard, J.G. (2000) Oncogenic Ras downregulates Rac activity, which leads to increased Rho activity and epithelial–mesenchymal transition. *J. Cell Biol.*, **149**, 775–781.

Submitted on May 9, 2002; accepted on August 14, 2002